Inorganic Chemistry

Article

pubs.acs.org/IC

Binding of β-Lactam Antibiotics to a Bioinspired Dizinc Complex Reminiscent of the Active Site of Metallo-β-lactamases

Simone Wöckel, Joanna Galezowska,† Sebastian Dechert, and Franc Meyer*

Institute of Inorganic Chemistry, Georg-August-University Göttingen, Tammannstrasse 4, 37077 Göttingen, Germany

Supporting Information

ABSTRACT: Metallo-β-lactamases (mβls) cause bacterial resistance toward a broad spectrum of β-lactam antibiotics by catalyzing the hydrolytic cleavage of the four-membered β-lactam ring, thus inactivating the drug. Minutiae of the mechanism of these enzymes are still not well understood, and reports about binding studies of the substrates to the enzymes as well as to synthetic model systems are rare. Here we report a new pyrazolate-based bioinspired dizinc complex (**1**) reminiscent of the active site of binuclear mβls. Since **1** does not mediate hydrolytic degradation of β-lactams, the binding of a series of common β-lactam antibiotics (benzylpenicillin, cephalotin, 6-aminopenicillanic acid, ampicillin) as well as the inhibitor sulbactam and the simplest β-lactam, 2-azetidinone, to the dizinc core of **1** could now be studied in detail by NMR and IR spectroscopy as well as mass spectrometry. X-ray crystallographic information was obtained for **1** and its complexes with 2-azetidinone (**2**) and sulbactam (**3**); the latter represents the first structurally characterized dizinc complex with a bound β-lactam drug. While 2-azetidinone was found deprotonated and bridging in the clamp of the two zinc ions in **2**, in **3** and all other cases the substrates preferentially bind via their carboxylate group within the bimetallic pocket. The relevance of this binding mode for mβls and consequences for the design of functional model systems are discussed.

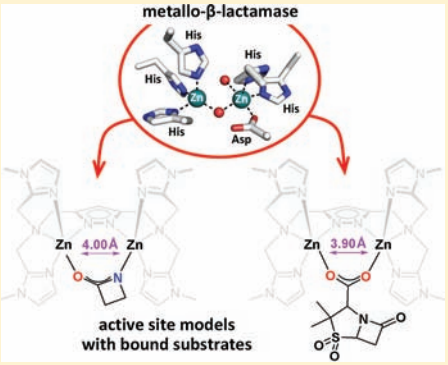

INTRODUCTION

Since the germ-killing effect of the strain *Penicillium notatum* was discovered by the bacteriologist Alexander Fleming[1] and a stable form of penicillin was isolated by Florey and Chain,[2] penicillins and related β-lactam compounds such as, for example, carbapenems and cephalosporins have developed into the most widely used class of antibiotics.[3] Their extensive and often excessive use for the treatment of bacterial diseases, however, has stimulated the pathogens to express enzymes that are able to defang these clinically important drugs. These enzymes known as β-lactamases hydrolytically cleave the C−N bond of the four-membered β-lactam ring, yielding the corresponding β-amino acid that is harmless to bacteria (Scheme 1).[4]

Scheme 1. C−N Bond Cleavage of β-Lactam Antibiotics by β-Lactamases

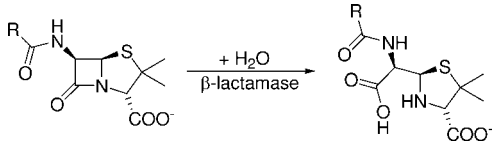

Members of one class of these enzymes (class B) contain at least one zinc ion in their active site and are therefore called metallo-β-lactamases (mβls);[5] this class is subdivided into three groups (B1, B2, and B3) depending on their amino acid sequence and zinc content.[6] Recently detected mβls such as the New Delhi mβls (NDM-1) confer nearly complete resistance to all standard intravenous β-lactam antibiotics and thus pose a major clinical threat.[7] Unfortunately, there are no effective inhibitors available so far for the emerging class B enzymes.

Members of the B1 and B3 mβls are most active as dizinc species.[8−10] The chemical surrounding of the zinc atoms within the active sites of most dizinc enzymes are rather similar and rich in histidines: one zinc atom is tetrahedrally coordinated by three histidines (3H-site) and a bridging water molecule, while the second zinc atom is hosted in a trigonal bipyramidal environment by one aspartate, one cysteine, one histidine (DCH-site for B1 enzymes), and two water molecules.[11] In type B3 enzymes the cysteine amino acid is replaced by an additional histidine resulting in a DHH-site for the second zinc atom. Details of the mechanisms of mono- and binuclear mβls were widely discussed in the literature[4,12−16] and still remain a controversial issue. It is generally accepted that the zinc ion acts as Lewis acid to interact with functional groups of the substrate and to decrease the pK_a of metal-bound water, generating the hydroxide nucleophile. More specifically, it is assumed that the carbonyl O-atom of the β-lactam ring binds to Zn1, while the carboxylate group of β-lactam antibiotics might coordinate to Zn2 that also stabilizes the N-atom leaving group.[11,17] This scenario is supported by structural information for several mβls

Received: November 11, 2011
Published: February 1, 2012

   dx.doi.org/10.1021/ic202425m | *Inorg. Chem.* 2012, 51, 2486−2493

with hydrolyzed substrates in their active sites, which shows both the N-atom of the cleaved β-lactam ring as well as a carboxylate-O bound to Zn2 in the enzyme−product complex.[18] Mechanistic studies of *Bacteroides fragilis* indicated that product formation and substrate consumption do not occur simultaneously, and an enzyme-bound intermediate was identified in which the leaving nitrogen atom stays negatively charged after C−N bond cleavage.[12,19,20] The proposed mechanism (Scheme 2) shows coordination of the substrate

Scheme 2. Proposed Mechanism of β-Lactam Cleavage Mediated by Dizinc mβls Such as NDM-1

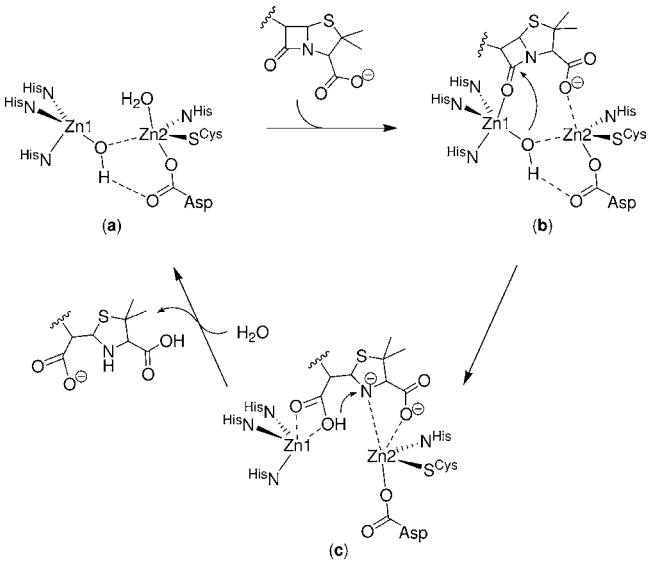

to both zinc atoms as the initial step. The asymmetrically bridging hydroxide acts as a nucleophile and attacks the carbonyl C-atom resulting in the cleavage of the C−N bond (**b**); the negatively charged N-atom is stabilized by Zn2 (**c**). This is followed by protonation of the N-atom (likely by the proton from the hydroxide nucleophile) and ligand exchange at Zn1 (**a**). The rate-determining step is proposed to be the breakdown of the intermediate.[12,17,19]

In recent years preorganized dizinc complexes have been developed as model systems for mβl active sites. Some of them showed catalytic activity in the hydrolysis of β-lactam substrates, which may help to understand the mechanistic pathways of the enzymes.[20−25] In addition, some insight into the binding modes of β-lactam substrates at mono- and dizinc sites could be obtained.[22−24,26,27] β-Lactam antibiotics like benzylpenicillin (pen, **a** in Chart 1) bear several potential donor groups that are able to coordinate to zinc atoms: (i) the carboxylate group, (ii) the lactam amide moiety, (iii) the thioether group, and (iv) the side-chain amide group.

Lippard and co-workers investigated the binding of benzylpenicillin and cephalotin (ceph, **b** in Chart 1) to binuclear zinc complexes derived from compartmental phenol- and naphthyridine ligands. From ^{13}C NMR and IR spectroscopy, monodentate coordination of the carboxylate group of the substrates to one of the zinc ions was proposed, while no interaction of the O-atom of the β-lactam amide with the metal ions could be observed.[22,23] Pyrazolate-based ligand scaffolds with chelating side arms attached to the 3- and 5-positions of the central heterocycle have proven well suited for emulating structural and functional characteristics of binuclear enzyme

Chart 1. Chemical Structures of Benzylpenicillin (pen, a), Cephalotin (ceph, b), Oxazetidinylacetate (oaa, c), and 2-Azetidinone (azet, d)

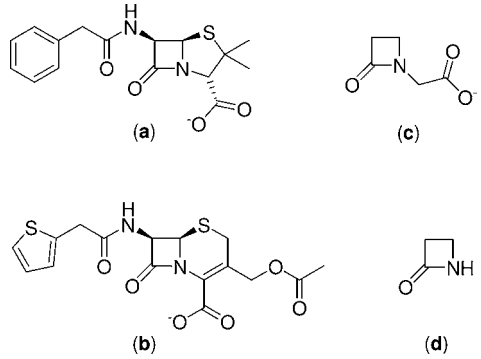

active sites.[28−30] When bound to a series of pyrazolate-bridged dizinc complexes the simple β-lactam derivate oxazetidinylacetate (oaa, **c** in Chart 1) that comprises both crucial groups, the β-lactam amide and the appended carboxylate group, revealed distinct binding modes depending on the number of vacant coordination sites. In all cases oaa was found bridging the two zinc ions via its carboxylate group, but additional involvement of the carbonyl O-atom of the β-lactam could also be achieved in an intermolecular fashion in a tetranuclear aggregate.[24] According to a CSD search, however, no model complex has yet been crystallographically characterized that features a genuine bicyclic β-lactam antibiotic bound to a zinc complex. Here we report a spectroscopic and mass-spectrometric study of the binding of some β-lactam antibiotics to a new bioinspired dizinc complex and the first X-ray crystal structure of a model complex that has the drug sulbactam bound within its bimetallic pocket. In addition, a dizinc complex with bridging parent β-lactamide is reported.

EXPERIMENTAL SECTION

General Experimental Considerations. The synthesis of **3** was performed under an anaerobic atmosphere of argon using standard Schlenk techniques. All other manipulations have been carried out in air using (p. A.) quality solvents. Et_2O was dried over sodium and MeCN over calcium hydride. 3,5-Bis[bis-((1-methyl-1*H*-imidazol-2-yl)-methyl)amine]-1*H*-pyrazole (HL) was synthesized as reported previously.[31] All other chemicals were purchased from commercial sources and used without further purification.

^1H and ^{13}C NMR spectra were recorded on Bruker Avance 300 or 500 MHz spectrometers; chemical shifts are reported in parts per million (ppm) relative to residual solvent signals of d_3-MeCN (1.94 ppm and 118.3 ppm) and d_6-acetone (2.05 ppm and 29.8 ppm). Electrospray ionization mass spectra (ESI-MS) were recorded on a Bruker HCT Ultra spectrometer. High resolution ESI-MS and FD-MS measurements were carried out by the central service department of the Institute for Organic and Biomolecular Chemistry at the University of Göttingen. Microanalyses were performed by the Analytical Laboratory of the Institute for Inorganic Chemistry of the University of Göttingen. IR spectra (as KBr pellets) were recorded using a Varian Digilab Excalibur FTS 3000 spectrometer.

Crystallography. The crystal data and details of the data collections are given in Table 1. X-ray data were collected on a STOE IPDS II diffractometer (graphite monochromated Mo Kα radiation, λ = 0.71073 Å) by use of ω scans at −140 °C. Structures were solved by direct methods and refined on F^2 using all reflections with SHELX-97.[32] Most non-hydrogen atoms were refined anisotropically. Hydrogen atoms were placed in calculated positions and assigned to an isotropic displacement parameter of 0.08 Å^2 (**2**) or 1.2/1.5 U_{eq}(C) (**1**, **3**). One ClO_4^- in **1** and **2** and acetonitrile solvent

dx.doi.org/10.1021/ic202425m | *Inorg. Chem.* 2012, 51, 2486−2493

Table 1. Crystal Data and Refinement Details for 1, 2, and 3

	1	2	3
empirical formula	$C_{33}H_{45}Cl_3N_{16}O_{12}Zn_2$	$C_{29}H_{41}Cl_2N_{13}O_{10}Zn_2$	$C_{39}H_{49}F_6N_{15}O_{11}S_3Zn_2$
formula weight	1094.94	933.39	1244.85
crystal size [mm^3]	0.5 × 0.25 × 0.17	0.50 × 0.45 × 0.37	0.50 × 0.50 × 0.28
crystal system	triclinic	monoclinic	monoclinic
space group	$P\bar{1}$	$C2/c$	$P2_1$
a [Å]	12.8010(7)	33.2454(7)	8.9165(3)
b [Å]	12.9777(7)	13.1917(4)	27.6888(6)
c [Å]	14.8777(7)	17.7362(4)	10.4972(3)
α [deg]	85.234(4)	90.00	90.00
β [deg]	76.122(4)	97.654(2)	96.022(2)
γ [deg]	84.947(4)	90.00	90.00
V [Å^3]	2385.2(2)	7709.1(3)	2577.32(13)
Z	2	8	2
ρ [g/cm^3]	1.525	1.608	1.604
$F(000)$	1124	3840	1276
μ [mm^{-1}]	1.246	1.454	1.145
T_{min}/T_{max}	0.5267/0.8066	0.5025/0.6068	0.5243/0.8057
θ range [deg]	1.64−27.04	1.66−26.72	1.47−25.62
hkl range	±16, −15 to 16, −19 to 18	±41, ±16, −22 to 19	±10, −32 to 33, ±12
measured refl.	21171	36574	32325
unique refl. [R_{int}]	10284 [0.0580]	8168 [0.0302]	9536 [0.0574]
observed refl. ($I > 2\sigma(I)$)	7865	7347	9331
data/restraints/param.	10284/32/642	8168/58/530	9536/3/695
goodness-of-fit (F^2)	0.939	1.092	1.033
$R1$, $wR2$ ($I > 2\sigma(I)$)	0.0448, 0.1193	0.0521, 0.1398	0.0421, 0.1119
$R1$, $wR2$ (all data)	0.0641, 0.1280	0.0581, 0.1433	0.0429, 0.1126
resid. el. dens. [e/Å^3]	−0.696/1.073	−0.587/1.915	−0.655/1.291

molecules in **1** were found to be disordered (occupancy factors ClO_4^- **1**: 0.619(6)/0.381(6), **2**: 0.383(2)/0.117(2); MeCN **1**: 0.281(6):/0.719(6)). SADI restraints (d_{Cl-O} and $d_{O\cdots O}$) and EADP constraints in case of **2** were used to model the disorder of the ClO_4^- anions. Atoms of the disordered solvent molecules and all oxygen atoms of the disordered ClO_4^- anion in **2** were refined isotropically. In the structure of **3** the sulfonyl group was found to be disordered about two positions (occupancy factors: 0.512(15)/0.488(15)). The two oxygen atoms of this group were refined isotropically. The largest residual electron density in **2** is found near the chlorine atoms of disordered perchlorate. The absolute structure parameter for **3**, 0.022(9), was determined with SHELXL-97 according to Flack.[33] The Face-indexed absorption corrections were performed numerically with the program X-RED.[34]

Synthesis of $[LZn_2(MeCN)_2](ClO_4)_3$ (1). To a solution of HL (200 mg, 0.40 mmol) in MeOH (20 mL), KOtBu (47 mg, 0.42 mmol) was added, and the mixture stirred at 33 °C until the solution became clear (~2 h). $Zn(ClO_4)_2{\cdot}6H_2O$ (298 mg, 0.80 mmol) was dissolved in MeOH (20 mL) and added dropwise to the ligand solution via a filter-pipet, whereby a colorless precipitate formed. The mixture was stirred for 2 h. After filtration, the solvent was evaporated, and the residue dissolved in MeCN (8 mL). Slow diffusion of Et_2O into the resulting solution of the crude product at room temperature (rt) afforded colorless crystals of **1**·2MeCN suitable for X-ray analysis. Yield: 274 mg (0.27 mmol, 68%). The bulk material persistently contains 1 equiv of $KClO_4$. Elem. Anal. Calcd for $C_{29}H_{39}Cl_3N_{14}O_{12}Zn_2{\cdot}KClO_4$: C 30.25, H 3.41, N 17.03. Found: C 30.70, H 3.52, N 17.19. ^{1}H NMR (300 MHz, rt, d_3-MeCN): δ 1.97 (s, 6H, MeCN), 3.59 (s, 12H, NMe), 4.00−4.12 (m, 12H, CH_2), 6.06 (s, 1H, CH^{Pz}), 7.10 (d, $^3J_{H,H}$ = 1.6 Hz, 4H, CH^{Imid}), 7.20 (d, $^3J_{H,H}$ = 1.5 Hz, 4H, CH^{Imid}). ^{13}C NMR (75 MHz, rt, d_3-MeCN): δ 1.7 ($\underline{C}H_3CN$), 33.6 (NMe), 51.0 (CH_2), 53.2 (CH_2), 100.8 (CH^{Pz}), 125.2 (CH^{Imid}), 125.3 (CH^{Imid}), 148.6 (C^{Imid}), 154.2 (C^{Pz}). MS (ESI+, MeCN): m/z (rel. intensity) = 827 (100) $[LZn_2(ClO_4)_2]^+$, 763 (9) $[LZn_2(H_3O_2)(ClO_4)]^+$, 364 (67) $[LZn_2(ClO_4)]^{2+}$, 332 (6) $[LZn_2(H_3O_2)]^{2+}$. IR (KBr, cm^{-1}): $\tilde{\nu}$ = 3144 (w), 2915 (w), 2020 (w), 1635 (m), 1546 (m), 1509 (s), 1447 (m), 1362 (m), 1281 (m), 1108 (vs, ClO_4), 960 (m), 876 (m), 751 (m), 656 (w), 626 (s).

Synthesis of $[LZn_2(azet_{-H})](ClO_4)_2$ (2). To a solution of the ligand HL (100 mg, 0.20 mmol) in MeOH (15 mL) were added 2 equiv of KOtBu (46 mg, 0.41 mmol) and 2 equiv of $Zn(ClO_4)_2{\cdot}6H_2O$ (146 mg, 0.39 mmol). The mixture was stirred at 40 °C for 1 h; afterward 1 equiv of 2-azetidinone (14.4 mg, 0.20 mmol) was added and stirring was continued for 2 h at rt. All volatile material was then evaporated under reduced pressure. The residue was taken up in a methanol/acetone mixture (10 mL, 9:1, v/v), and the solution after filtration was layered with light petroleum to gradually yield colorless crystals of **2**·MeOH over a period of several days. Yield: 52 mg (0.06 mmol, 28%). ^{1}H NMR (300 MHz, rt, d_6-acetone): δ 3.52 (m, 2H, CH_2^{azet}), 3.56 (m, 2H, CH_2^{azet}), 3.74 (s, 12H, NMe), 4.09 (s, 2H, CH_2), 4.16 (s, 2H, CH_2), 4.23 (s, 2H, CH_2), 4.29 (s, 4H, CH_2), 4.35 (s, 2H, CH_2), 6.15 (s, 1H CH^{Pz}), 7.08 (d, $^3J_{H,H}$ = 1.5 Hz, 2H, CH^{Imid}), 7.12 (d, $^3J_{H,H}$ = 1.5 Hz, 2H, CH^{Imid}), 7.32 (d, $^3J_{H,H}$ = 1.5 Hz, 2H, CH^{Imid}), 7.33 (d, $^3J_{H,H}$ = 1.5 Hz, 2H, CH^{Imid}). ^{13}C NMR (75 MHz, rt, d_6-acetone): δ 33.2 (NMe), 36.2 (CH_2^{azet}), 39.5 (CH_2^{azet}), 50.9 (CH_2), 51.4 (CH_2), 101.9 (CH^{Pz}), 124.8 (CH^{Imid}), 125.3 (CH^{Imid}), 125.6 (CH^{Imid}), 148.8 (C^{Imid}), 152.5 (C^{Pz}) ppm; $C{=}O^{azet}$ not observed. MS (FD+): m/z (rel. intensity) = 798 (77) $[LZn_2(C_3H_4NO)(ClO_4)]^+$, 350 (100) $[LZn_2(C_3H_4NO)]^{2+}$. HR-MS (ESI+) Calcd (m/z) for $[C_{28}H_{37}N_{13}O_5ClZn_2]^+$: 798.1307. Found: 798.1300. Calcd (m/z) for $[C_{28}H_{37}N_{13}OZn_2]^{2+}$: 349.5908. Found: 349.5915. IR (KBr, cm^{-1}): $\tilde{\nu}$ = 3128 (w), 2951 (w), 2920 (w), 1736 (m), 1632 (s), 1545 (w), 1509 (s), 1414 (m), 1360 (m), 1284 (m), 1222 (w), 1096 (vs, ClO_4), 978 (m), 961 (m), 878 (w), 753 (m), 624 (s).

Synthesis of $[LZn_2(sul)](SO_3CF_3)_2$ (3). HL (100 mg, 0.20 mmol), KOtBu (22 mg, 0.20 mmol), $Zn(SO_3CF_3)_2$ (145 mg, 0.40 mmol), and sulbactam sodium salt (51 mg, 0.20 mmol) were dried in vacuum. Dry MeCN (8 mL) was added, and the suspension was stirred for 3 d resulting in an almost clear solution. Filtration via cannula and slow diffusion of Et_2O into the MeCN solution afforded colorless crystals of **3**·2MeCN suitable for X-ray crystallography. Yield: 36 mg (0.03 mmol,

dx.doi.org/10.1021/ic202425m | Inorg. Chem. 2012, 51, 2486−2493

15%). ^{1}H NMR (300 MHz, rt, d_3-MeCN): δ 1.73 (s, 3H, Me^{sul}), 1.76 (s, 3H, Me^{sul}), 3.34−3.61 (m, 14H, NMe and CH$_2^{sul}$), 3.99−4.15 (m, 12H, CH$_2$), 4.73 (s, 1H, CHCOO^{sul}), 4.95 (dd, $^3J_{H,H}$ = 4.5 Hz, $^3J_{H,H}$ = 1.9 Hz, 1H, CHCH$_2^{sul}$), 6.14 (s, 1H, CH^{Pz}), 6.98 (d, $^3J_{H,H}$ = 1.5 Hz, 2H, CH^{Imid}), 7.00 (d, $^3J_{H,H}$ = 1.5 Hz, 2H, CH^{Imid}), 7.12 (bs, 4H, CH^{Imid}). ^{13}C NMR (75 MHz, rt, d_3-MeCN), assignment based on HSQC/HBMC experiments: δ 18.9 (Me^{sul}), 21.2 (Me^{sul}), 33.6 (NMe), 38.5 (CH$_2^{sul}$), 51.6 (CH$_2$), 51.7 (CH$_2$), 53.8 (CH$_2$), 62.2 (CHCH$_2^{sul}$), 64.0 (SC^{sul}), 66.5 (CHCOO^{sul}), 102.3 (CH^{Pz}), 125.0 (CH^{Imid}), 125.1 (CH^{Imid}), 125.4 (CH^{Imid}), 125.5 (CH^{Imid}), 148.7 (C^{Imid}), 148.8 (C^{Imid}), 152.7 (C^{Pz}), 173.6 (C=O^{sul}), 175.3 (COO^{sul}). MS (ESI+, MeCN): m/z (rel. intensity) = 1010 (28) [LZn$_2$(sul)(SO$_3$CF$_3$)]$^+$, 430 (100) [LZn$_2$(sul)]$^{2+}$. HR-MS (ESI+) Calcd (m/z) for [C$_{34}$H$_{43}$F$_3$N$_{13}$O$_8$S$_2$Zn$_2$]$^+$: 1010.1329. Found: 1010.1335. Calcd (m/z) for [C$_{33}$H$_{43}$N$_{13}$O$_5$SZn$_2$]$^{2+}$: 430.5901. Found: 430.5903. IR (KBr, cm^{-1}): $\tilde{\nu}$ = 3130 (w), 2923 (w), 2863 (w), 1790 (s), 1625 (vs), 1548 (w), 1510 (s), 1424 (s), 1359 (m), 1320 (m), 1264 (vs), 1225 (m), 1160 (s), 1118 (m), 1031 (vs), 983 (m), 959 (m), 875 (m), 791 (m), 756 (m), 710 (w), 676 (w), 639 (s), 571 (m), 518 (m).

RESULTS AND DISCUSSION

The ligand HL was used in this study (Chart 2),[31] since it provides two binding pockets rich in imidazole donors,

Chart 2. Chemical Structures of Ligand HL and Complex 1

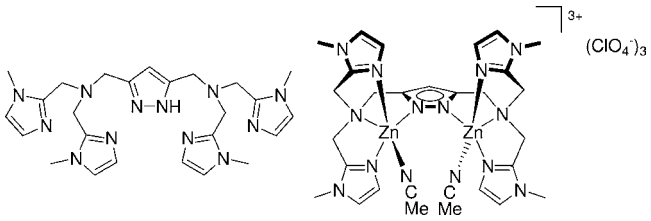

HL 1

somewhat reminiscent of the predominant histidine coordination in mβls (though not exactly reflecting the distinct pockets and the asymmetry of the natural archetype). Zn···Zn separations in the {LZn$_2$} scaffold were found to be variable between 3.4 and 4.2 Å,[35] which is similar to the plasticity found for the native enzyme active sites. Complex [LZn$_2$(MeCN)$_2$](ClO$_4$)$_3$ (**1**) that has two labile MeCN solvent molecules serves as the precursor to investigate the binding of a variety of β-lactam antibiotic drugs to a dizinc core: benzylpenicillin (penicillin G, pen), cephalotin (ceph), 6-aminopenicillanic acid (6-apa), and ampicillin (amp); their chemical structures are depicted in Charts 1 and 3. In addition, 2-azetidinone (azet,

Chart 3. Chemical Structures of Sulbactam (sul), 6-Aminopenicillanic Acid (6-apa), and Ampicillin (amp) That Have Been Used for Binding Studies in This Work

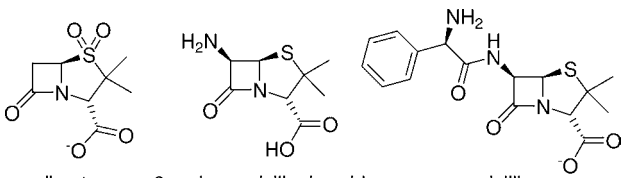

sulbactam (sul) 6-aminopenicillanic acid (6-apa) ampicillin (amp)

Chart 1) and sulbactam (sul; Chart 3) were chosen as substrates. Sulbactam has no bactericidal function in medicine, but it irreversibly binds to the active sites of many lactamases and thus inhibits their hydrolytic activity. Because of its hydrolytic stability toward β-lactamases, sul deemed to be a particularly suitable substrate for the present studies.

Synthesis of the Dizinc Scaffold. Treating HL with 1 equiv KOtBu and 2 equiv of Zn(ClO$_4$)$_2$·6H$_2$O resulted, after crystallization from acetonitrile, in the formation of [LZn$_2$(MeCN)$_2$](ClO$_4$)$_3$ (**1**). This complex crystallizes as **1**·2MeCN in the triclinic space group $P\bar{1}$ with two molecules per unit cell; the molecular structure of the cation is shown in Figure 1.

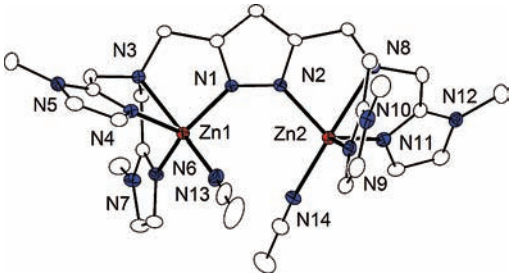

Figure 1. Molecular structure of the cation of **1** (thermal ellipsoids drawn at the 30% probability level). Hydrogen atoms, counterions and solvent molecules have been omitted for clarity. Selected bond lengths [Å] and angles [deg] for **1**: Zn1−N1 2.005(3), Zn1−N6 2.006(3), Zn1−N4 2.030(3), Zn1−N13 2.066(3), Zn1−N3 2.376(2), Zn2−N2 1.996(2), Zn2−N9 2.002(3), Zn2−N11 2.018(3), Zn2−N14 2.069(3), Zn2−N8 2.396(3), Zn1···Zn2 4.1028(5); N1−Zn1−N6 113.15(10), N1−Zn1−N4 118.50(10), N6−Zn1−N4 111.48(11), N1−Zn1−N13 107.56(11), N6−Zn1−N13 109.55(12), N4−Zn1−N13 94.67(11), N1−Zn1−N3 75.09(9), N6−Zn1−N3 77.46(10), N4−Zn1−N3 75.74(9), N13−Zn1−N3 169.90(11), N2−Zn2−N9 109.71(10), N2−Zn2−N11 120.73(10), N9−Zn2−N11 113.06(10), N2−Zn2−N14 104.81(11), N9−Zn2−N14 110.50(12), N11−Zn2−N14 96.59(11), N2−Zn2−N8 75.56(10), N9−Zn2−N8 77.05(10), N11−Zn2−N8 76.21(9), N14−Zn2−N8 171.39(10).

In **1** each zinc atom is ligated by one pyrazole N-atom, two imidazole N-atoms, and the tertiary amine nitrogen atom. In addition, two acetonitrile ligands fill the central binding sites, resulting in a distorted trigonal bipyramidal coordination polyhedron of both zinc atoms (Zn1: τ_5 = 0.86, Zn2: τ_5 = 0.84).[36] The zinc−zinc separation is 4.10 Å. ESI-MS analysis of **1** from acetonitrile solutions showed the formation of two species: fragments [LZn$_2$(ClO$_4$)$_2$]$^+$ (at m/z = 827) and [LZn$_2$(ClO$_4$)]$^{2+}$ (at m/z = 364) can likely be assigned to **1** after loss of the MeCN ligands and some of the perchlorate counterions. In addition, fragments at m/z = 763 and 332 with isotopic distribution pattern characteristic of [LZn$_2$(H$_3$O$_2$)(ClO$_4$)]$^+$ and [LZn$_2$(H$_3$O$_2$)]$^{2+}$, respectively, suggest that species with an anionic HOH···OH bridge in the bimetallic pocket can be formed under electrospray conditions. The propensity of related pyrazolate-based bimetallic scaffolds to incorporate a H$_3$O$_2$ bridge has been observed previously.[37]

Binding of β-Lactams. In an initial experiment complex **1** prepared in situ was treated with the simplest β-lactam, 2-azetidinone. Both ESI and FD mass spectrometry of the isolated product **2** showed major signals at m/z = 350 (for [LZn$_2$(C$_3$H$_4$NO)]$^{2+}$), and 798 (for [LZn$_2$(C$_3$H$_4$NO)(ClO$_4$)]$^+$), both confirmed by high resolution (HR) MS, suggesting that 2-azetidinone is bound in its deprotonated form. IR spectroscopy of **2** revealed a strong band at 1632 cm^{-1} assigned to the β-lactam ν(C=O) amide stretch, which represents a significant shift compared to free 2-azetidinone (IR: 1723 cm^{-1}; Raman: 1697 cm^{-1})[38,39] and indicates an N,O-

dx.doi.org/10.1021/ic202425m | Inorg. Chem. 2012, 51, 2486−2493

bridging binding mode that we have observed before for this particular substrate.[26] The molecular structure of **2** was finally verified by X-ray crystallography on single crystals that were obtained from a methanol/acetone solution layered with light petroleum (Figure 2).

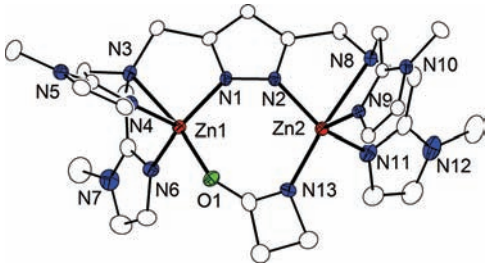

Figure 2. Molecular structure of the cation of **2** (thermal ellipsoids drawn at the 30% probability level). Hydrogen atoms, counterions and solvent molecules have been omitted for clarity. Selected bond lengths [Å] and angles [deg] for **2**: Zn1–N1 2.008(3), Zn1–N4 2.021(3), Zn1–O1 2.022(3), Zn1–N6 2.034(3), Zn1–N3 2.403(3), Zn2–N13 1.996(4), Zn2–N2 2.003(3), Zn2–N9 2.017(3), Zn2–N11 2.043(4), Zn2–N8 2.483(3), Zn1···Zn2 3.9952(6); N1–Zn1–N4 116.39(13), N1–Zn1–O1 112.37(12), N4–Zn1–O1 99.25(12), N1–Zn1–N6 112.71(13), N4–Zn1–N6 114.21(13), O1–Zn1–N6 99.77(13), N1–Zn1–N3 76.52(12), N4–Zn1–N3 76.07(12), O1–Zn1–N3 171.11(12), N6–Zn1–N3 75.78(12), N13–Zn2–N2 110.48(14), N13–Zn2–N9 104.19(15), N2–Zn2–N9 113.71(12), N13–Zn2–N11 101.23(16), N2–Zn2–N11 116.36(14), N9–Zn2–N11 109.49(13), N13–Zn2–N8 174.58(13), N2–Zn2–N8 74.51(12), N9–Zn2–N8 75.01(12), N11–Zn2–N8 74.24(14).

Apparently the presence of an NH group in N-unsubstituted β-lactams results in deprotonation and preferential incorporation of anionic β-lactamide within the clamp of the two zinc ions. This leads to a shortening of the C–N bond (1.286(6) Å) and elongation of the C=O bond (1.273(5) Å) compared to free 2-azetidinone (1.333(2) and 1.226(2) Å, respectively).[40] It should be noted that structurally characterized examples of complexes with bridging β-lactamide are generally scarce,[41] and **2** is only the second example in zinc chemistry.[26] Clearly this coordination of the β-lactam moiety is different from the binding of N-substituted β-lactam derivatives such as the antibiotics mentioned above, both in the enzyme active sites and in model systems.

As revealed by NMR and IR spectroscopy, treatment of **1** with pen, ceph, sul, 6-apa, and amp does not lead to ring cleavage and degradation of the substrates over a period of two weeks, which allowed studying their binding to the dizinc core $\{LZn_2\}$ in more detail. Here the results are presented for benzylpenicillin (pen) and sulbactam (sul) as representative substrates, but findings are basically similar for all other substrates as well (see the Supporting Information).

ESI-MS Studies. Equimolar amounts of **1** and pen were mixed in acetonitrile, and the solution was stirred until all components dissolved and finally filtered. ESI-MS measurements revealed signals at m/z = 481 and 1061 with isotopic distribution patterns characteristic for fragments $[LZn_2(pen)]^{2+}$ (A) and $[LZn_2(pen)(ClO_4)]^+$ (B), respectively, as it is shown in Figure 3.

Assignment of fragments A and B was additionally confirmed by HR-MS analysis (m/z calc. 481.1217, found 481.1216 for $[C_{41}H_{50}N_{14}O_4SZn_2]^{2+}$; m/z calc. 1061.1923, found 1061.1923 for $[C_{41}H_{50}ClN_{14}O_8SZn_2]^+$). While ESI-MS thus clearly

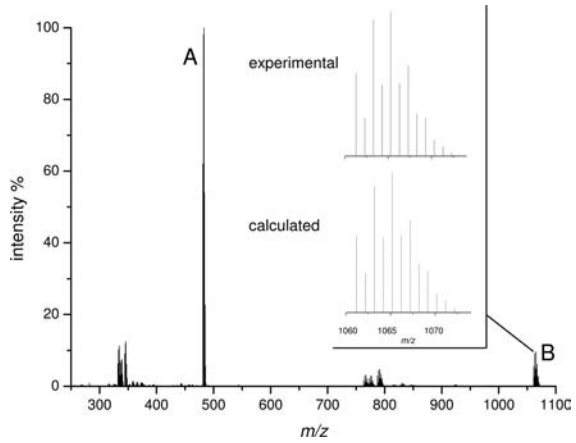

Figure 3. ESI-MS spectrum of a mixture of **1** and pen (ratio 1:1) in MeCN; $[LZn_2(pen)]^{2+}$ (A), $[LZn_2(pen)(ClO_4)]^+$ (B), the inset shows the experimental and calculated isotopic distribution for fragment B.

showed the coordination of pen and sul (as well as ceph, 6-apa, and amp) to **1**, we had to turn to NMR and IR spectroscopy to provide information about which functional groups are involved in metal ion binding.

NMR Studies. NMR measurements were carried out in d_3-MeCN/D_2O (9:1, v/v) at room temperature (some D_2O was necessary for complete dissolution of pen). Completeness of the reaction was confirmed by diffusion-ordered (DOSY) NMR: combining equimolar amounts of **1** and pen in an NMR tube showed the formation of only one species (adduct) that is larger than both starting materials, without any residual peaks of either **1** or pen. Figure 4 shows the ^{1}H NMR spectra of **1** (upper row), pen (bottom row), and an equimolar mixture of both (middle).

The most pronounced shift is observed for H-2 close to the carboxylate group, namely, from 4.07 ppm (pen) to 4.82 ppm (**1**/pen). Protons of the two methyl groups (H-9/10) also undergo a downfield shift from 1.46/1.52 ppm to 1.68/1.80 ppm, while changes for all other signals are minor. ^{13}C NMR resonances were assigned by 2D HSQC and HMBC experiments. Comparing the HMBC spectrum of pen with the adduct spectrum, a significant shift of the quaternary carbon atom of the carboxylate group (C-8) to lower field is obvious (from 173.3 to 175.5 ppm). For a complete listing of NMR chemical shifts see the Supporting Information. NMR spectroscopy thus suggested binding of pen via its carboxylate group to the zinc ions of **1**.

IR Spectroscopy. Different carboxylate binding modes (ionic, monodentate, bidentate chelating, or bridging) give rise to distinct relative frequencies for the asymmetric and symmetric COO^- vibrations, and the separation $\Delta\tilde{\nu} = \tilde{\nu}_{asym}(COO^-) - \tilde{\nu}_{sym}(COO^-)$ is an often used criterion to distinguish between them.[42] Values for the relevant vibrational bands are listed in Table 2 and show a difference ($\Delta\tilde{\nu}$) of 191 cm^{-1} for $[LZn_2(pen)](ClO_4)_2$. While this value is not unambiguous, it has been stated that virtually all complexes with $\Delta\tilde{\nu}$ in the range 150–200 cm^{-1} have chelating and/or bridging acetate groups.[42a] A considerable change, however, was also noticed for the side-chain amide C=O vibration band, which was observed as a broad shoulder in the spectrum of the adduct **1**/pen. It is known from literature that the position of the amide band for pen salts can differ depending on the cation (1669 cm^{-1} for the potassium salt and 1700 cm^{-1} for the

dx.doi.org/10.1021/ic202425m | Inorg. Chem. 2012, 51, 2486–2493

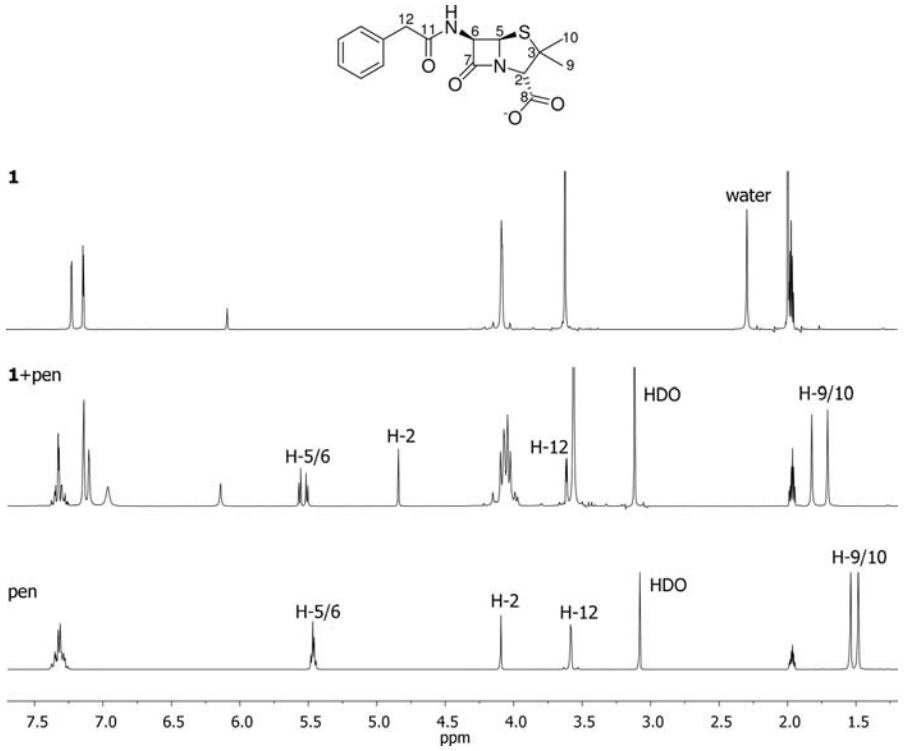

Figure 4. ^{1}H NMR spectra of **1** in d_3-MeCN (upper spectrum), an equimolar mixture of **1** and pen (middle), and pen (bottom) in d_3-MeCN/D_2O (9:1, v/v). The numbering scheme for pen is included.

Table 2. Relevant Vibrational Bands of Free and Coordinated Substrates pen and sul[a]

compound	$\tilde{\nu}$(CO) lactam	$\tilde{\nu}$(CO) amide	$\tilde{\nu}_{asym}$(COO)	$\tilde{\nu}_{sym}$(COO)	$\Delta\tilde{\nu}_{(asym-sym)}$
[K(pen)]	1772	1670	1613	1396	217
$[LZn_2(pen)](ClO_4)_2$	1776	1647 (sh)	1612	1421	191
[Na(sul)]	1773		1604	1399	205
$[LZn_2(sul)](SO_3CF_3)_2$	1790		1625	1424	201

[a] $\tilde{\nu}$ is given in cm^{-1}.

sodium salt).[43] In addition, the amide vibration of penicilloic acid appears at 1645 cm^{-1}.[43] Changes of the position of this band are thus not fully conclusive. However, since the ^{13}C NMR resonance of the amide group (C-11) does not change compared to free pen, coordination of pen via its amide group is deemed unlikely for the **1**/pen system.

Molecular Structure of $[LZn_2(sul)](SO_3CF_3)_2$ (3). Crystallization of adducts of **1** and pen (as well as adducts of **1** and ceph, 6-apa, and amp) did not lead to crystalline material so far, but rather resulted in colorless oils. However, single crystals suitable for X-ray diffraction could be obtained from the reaction of HL, KO^{t}Bu, and $Zn(SO_3CF_3)_2$ with sulbactam (sul) sodium salt, which also bears the structural motif of a thia-azabicycloheptanone alike to the various β-lactam antibiotics. $[LZn_2(sul)](SO_3CF_3)_2$ (**3**) crystallizes in the monoclinic space group $P2_1$ with two formula units per unit cell; the molecular structure of its cation is shown in Figure 5, together with selected atom distances and bond angles.

The molecular structure of **3** illustrates that the sulbactam substrate is hosted in the bimetallic pocket of the $\{LZn_2\}$ scaffold and exhibits the μ-η^1:η^1 binding mode of the carboxylate moiety that was deduced from spectroscopic data. The Zn···Zn separation of 3.90 Å is shorter than in **1** (4.10 Å) and slightly shorter than in **2** (4.00 Å), reflecting some degree of plasticity that allows the bimetallic core to adapt to the requirements of the exogenous ligands. The zinc atoms in **3** are located within the pyrazolato plane, while the carboxylate moiety of sulbactam is displaced slightly out of this plane (d(O1···pz) = 0.17(1) Å, d(O2···pz) = 0.31(1) Å, and d(C26···pz) = 0.41(1) Å). The sulfonyl group of the substrate was found to be disordered (not shown in Figure 5) and neither the sulfonyl group nor the amide-O of the β-lactam ring is involved in any coordination to the zinc atoms.

Comparing ^{1}H NMR spectra of **3** and free sulbactam, the most pronounced downfield shift is observed for H-2 (numbering as for pen, see Figure 4), namely, from 4.00 to 4.73 ppm. In addition, the signals of the methyl protons (H-9/10) are shifted to lower field (from 1.37 and 1.50 ppm to 1.73 and 1.76 ppm, respectively), just as it is also observed for all the other substrates. ^{13}C NMR spectroscopy reveals a significant shift of the C-8 signal (from 172.5 to 175.3 ppm). All these findings are in accordance with the results obtained with pen and corroborate the coordination of all β-lactam substrates investigated here via μ-η^1:η^1 carboxylate binding to the two zinc atoms of the $\{LZn_2\}$ skeleton, as revealed by X-ray analysis in the case of sulbactam. NMR spectroscopy also confirms that sulbactam is tightly bound in solution, since the two side arms of the ligand L become inequivalent in the adduct

dx.doi.org/10.1021/ic202425m | Inorg. Chem. 2012, 51, 2486−2493

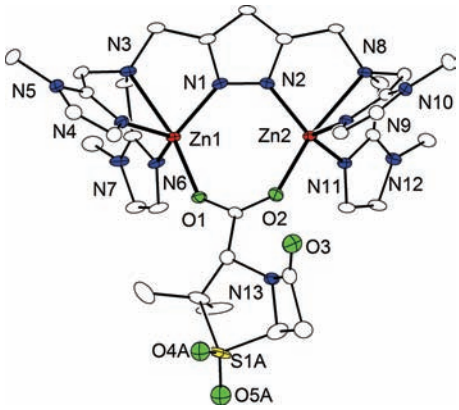

Figure 5. Molecular structure of the cation of **3** (thermal ellipsoids drawn at the 30% probability level). Hydrogen atoms, counterions, and solvent molecules have been omitted for clarity. Selected bond lengths [Å] and angles [deg] for **3**: Zn1–N1 1.981(3), Zn1–N6 1.995(3), Zn1–N4 1.998(4), Zn1–O1 2.027(3), Zn1–N3 2.471(3), Zn2–N2 1.981(3), Zn2–N9 2.011(4), Zn2–O2 2.011(3), Zn2–N11 2.014(3), Zn2–N8 2.440(3), Zn1···Zn2 3.9010(6); N1–Zn1–N6 113.72(14), N1–Zn1–N4 109.70(14), N6–Zn1–N4 119.50(15), N1–Zn1–O1 114.13(12), N6–Zn1–O1 99.69(12), N4–Zn1–O1 98.77(13), N1–Zn1–N3 76.24(12), N6–Zn1–N3 76.16(12), N4–Zn1–N3 75.58(13), O1–Zn1–N3 169.55(12), N2–Zn2–N9 113.17(13), N2–Zn2–O2 114.60(13), N9–Zn2–O2 97.55(13), N2–Zn2–N11 109.93(13), N9–Zn2–N11 119.81(14), O2–Zn2–N11 100.59(13), N2–Zn2–N8 76.26(12), N9–Zn2–N8 75.35(12), O2–Zn2–N8 168.95(12), N11–Zn2–N8 76.40(12).

$[LZn_2(sul)]^{2+}$. For example, two ^{1}H NMR signals, each representing four H atoms, are found for the imidazole-bound protons of $[LZn_2(MeCN)_2]^{3+}$, while three signals of intensities 2:2:4 are observed for **3**. Likewise, four ^{13}C NMR resonances are detected for the imidazole-CH of **3**. The rather large and inconclusive $\Delta\tilde{\nu}$ = 201 cm^{-1} for **3**, which is only slightly lower than for the sulbactam sodium salt (205 cm^{-1}), shows that care should be taken when correlating such IR data with potential carboxylate binding modes.

CONCLUSIONS

The present $\{LZn_2\}$ scaffold that provides two imidazole-rich metal-ion binding compartments appears to be suitable for emulating some structural features of the active site of dizinc metallo-β-lactamases. $\{LZn_2\}$ exhibits sufficient plasticity with respect to the Zn···Zn separation and does not promote the hydrolytic cleavage of β-lactam substrates, which has allowed for a detailed spectroscopic study of the substrate binding mode and even for the first crystallographic characterization of a dizinc complex with a bound customary β-lactam, sulbactam. Cationic complexes such as $[LZn_2(MeCN)_2]^{3+}$ evidently have a high tendency to accommodate anionic coligands within the bimetallic pocket, which in this case leads to the deprotonation and bridging coordination of 2-azetidinone as well as to the preferred binding of all studied β-lactam antibiotics via their carboxylate groups. Provided that the given Zn···Zn distance is compatible with μ-η^1:η^1 carboxylate coordination, it is likely that such substrate binding does also prevail in all other dizinc model complexes studies thus far.[21] This has important implications for the development of functional model systems, since it positions the β-lactam amide moiety relatively far (and perhaps unfavorably) from the dizinc site and requires additional accessible coordination sites for generating a metal-bound hydroxide nucleophile.

The situation encountered in **3** thus differs from what is proposed for the substrate binding in dizinc metallo-β-lactamases. On the basis of structural evidence and computational modeling, recent scenarios assume carboxylate coordination to only one of the metal ions in the enzyme active sites. Additional residues in the enzyme active site pocket clearly play a major role in positioning the substrate for nucleophilic attack and ring-opening. While it remains a quite demanding task to emulate any protein-like second sphere in synthetic small-molecule complexes, cationic groups or proper hydrogen-bonding sites appended in the periphery of the ligand scaffold may serve as suitable anchors for the carboxylate group, thus preventing the bridging carboxylate coordination mode. Some ligand scaffolds of that type have been developed in recent years[44,45] and may prove valuable for future modeling of the metallo-β-lactamase active site.

ASSOCIATED CONTENT

Supporting Information

Table of relevant IR bands of free and coordinated ceph, 6-apa, and amp. ^{1}H NMR spectra as well as ^{1}H and ^{13}C NMR chemical shifts of **1**/pen, pen, sul, **1**/ceph, ceph, **1**/6-apa **1**/6-apa+KO^{t}Bu, **1**/amp, and amp. ESI-MS spectra of **1**/ceph, **1**/6-apa, **1**/amp, and **3**. This material is available free of charge via the Internet at http://pubs.acs.org.

AUTHOR INFORMATION

Corresponding Author

*E-mail: franc.meyer@chemie.uni-goettingen.de. Fax: +49 551 393063. Phone: +49 551 393012.

Present Address

[†]Department of Inorganic Chemistry, Faculty of Pharmacy, Wroclaw Medical University, Szewska 38, 50-139 Wroclaw, Poland.

ACKNOWLEDGMENTS

Financial support by the Deutsche Forschungsgemeinschaft (International Research Training Group 1422 "Metal Sites in Biomolecules: Structures, Regulation and Mechanisms"; see www.biometals.eu) is gratefully acknowledged. J.G. would like to thank the Alexander von Humboldt Foundation (post-doctoral fellowship) and the Foundation for Polish Science for support. We thank Dr. Holm Frauendorf (Institute of Organic and Biomolecular Chemistry at the Georg-August-University) for collecting HR ESI-MS and FD-MS data.

REFERENCES

(1) Fleming, A. *Br. Med. Bull.* **1944**, *2*, 4–5.
(2) Chain, E.; Florey, H. W.; Gardner, A. D.; Heatley, N. G.; Jennings, M. A.; Orr-Ewing, J.; Sanders, A. G. *Lancet* **1940**, 226–228.
(3) von Nussbaum, F.; Brands, M.; Hinzen, B.; Weigand, S.; Häbich, D. *Angew. Chem.* **2006**, *118*, 5194–5254.
(4) Page, M. I.; Laws, A. P. *Chem. Commun.* **1998**, 1609–1617.
(5) Bebrone, C. *Biochem. Pharmacol.* **2007**, *74*, 1686–1701.
(6) Galleni, M.; Lamotte-Brasseur, J.; Rossolini, G. M.; Spencer, J.; Dideberg, O.; Frére, J.-M. *Antimicrob. Agents Chemother.* **2001**, *45*, 660–663.
(7) Cornaglia, G.; Giamarellou, H.; Rossolini, G. M. *Lancet Infect. Dis.* **2011**, *11*, 381–393.
(8) Badarau, A.; Page, M. I. *J. Biol. Inorg. Chem.* **2008**, *13*, 919–928.

(9) Jacquin, O.; Balbeur, D.; Damblon, C.; Marchot, P.; De Pauw, E.; Roberts, G. C. K.; Frère, J.-M.; Matagne, A. *J. Mol. Biol.* **2009**, *392*, 1278−1291.
(10) Hu, Z.; Periyannan, G.; Bennett, B.; Crowder, M. W. *J. Am. Chem. Soc.* **2008**, *130*, 14207−14216.
(11) Fabiane, S. M.; Sohi, M. K.; Wan, T.; Payne, D. J.; Bateson, J. H.; Mitchell, T.; Sutton, B. J. *Biochemistry* **1998**, *37*, 12404−12411.
(12) Wang, Z.; Fast, W.; Benkovic, S. J. *Biochemistry* **1999**, *38*, 10013−10023.
(13) Crowder, M. W.; Spencer, J.; Vila, A. J. *Acc. Chem. Res.* **2006**, *39*, 721−728.
(14) Bounaga, S.; Laws, A. P.; Galleni, M.; Page, M. I. *Biochem. J.* **1998**, *331*, 703−711.
(15) Wang, Z.; Fast, W.; Valentine, A. M.; Benkovic, S. J. *Curr. Opin. Chem. Biol.* **1999**, *3*, 614−622.
(16) Page, M. I.; Badarau, A. *Bioinorg. Chem. Appl.* **2008**, Article 576297 DOI: 10.1155/2008/576297.
(17) (a) Suarez, D.; Diaz, N.; Merz, K. M. Jr. *J. Comput. Chem.* **2002**, *23*, 1587−1600. (b) Xu, D.; Guo, H.; Cui, Q. *J. Am. Chem. Soc.* **2007**, *129*, 10814−10822. (c) Wang, J.-F.; Chou, K.-C. *PLoS ONE* **2011**, *6*, e18414.
(18) (a) Spencer, J.; Read, J.; Sessions, R. B.; Howell, S.; Blackburn, G. M.; Gamblin, S. J. *J. Am. Chem. Soc.* **2005**, *127*, 14439−14444. (b) Zhang, H.; Hao, Q. *FASEB J.* **2011**, *25*, 2574−2582.
(19) Wang, Z.; Fast, W.; Benkovic, S. J. *J. Am. Chem. Soc.* **1998**, *120*, 10788−10789.
(20) Kaminskaia, N. V.; Spingler, B.; Lippard, S. J. *J. Am. Chem. Soc.* **2001**, *123*, 6555−6563.
(21) (a) Tamilselvi, A.; Mugesh, G. *J. Biol. Inorg. Chem.* **2008**, *13*, 1039−1053. (b) Umayal, M.; Tamilselvi, A.; Mugesh, G. *Prog. Inorg. Chem.* **2012**, *57*, 395−443.
(22) Kaminskaia, N. V.; Spingler, B.; Lippard, S. J. *J. Am. Chem. Soc.* **2000**, *122*, 6411−6422.
(23) Kaminskaia, N. V.; He, C.; Lippard, S. J. *Inorg. Chem.* **2000**, *39*, 3365−3373.
(24) Bauer-Siebenlist, B.; Dechert, S.; Meyer, F. *Chem.—Eur. J.* **2005**, *11*, 5343−5352.
(25) (a) Tamilselvi, A.; Nethaji, M.; Mugesh, G. *Chem.—Eur. J.* **2006**, *12*, 7797−7806. (b) Umayal, M.; Mugesh, G. *Inorg. Chim. Acta* **2011**, *372*, 353−361.
(26) Meyer, F.; Pritzkow, H. *Eur. J. Inorg. Chem.* **2005**, 2346−2351.
(27) Gross, F.; Vahrenkamp, H. *Inorg. Chem.* **2005**, *44*, 4433−4440.
(28) Klingele, J.; Dechert, S.; Meyer, F. *Coord. Chem. Rev.* **2009**, *253*, 2698−2741.
(29) Meyer, F. *Eur. J. Inorg. Chem.* **2006**, 3789−3800.
(30) (a) Buchler, S.; Meyer, F.; Kaifer, E.; Pritzkow, H. *Inorg. Chim. Acta* **2002**, *337*, 371−386. (b) Ackermann, J.; Meyer, F.; Kaifer, E.; Pritzkow, H. *Chem.—Eur. J.* **2002**, *8*, 247−258. (c) Bauer-Siebenlist, B.; Meyer, F.; Farkas, E.; Vidovic, D.; Cuesta-Seijo, J. A.; Herbst-Irmer, R.; Pritzkow, H. *Inorg. Chem.* **2004**, *43*, 4189−4202. (d) Bauer-Siebenlist, B.; Meyer, F.; Farkas, E.; Vidovic, D.; Dechert, S. *Chem.—Eur. J.* **2005**, *11*, 4349−4360. (e) Penkova, L. V.; Maciag, A.; Rybak-Akimova, E. V.; Haukka, M.; Pavlenko, V. A.; Iskenderov, T. S.; Kozlowski, H.; Meyer, F.; Fritsky, I. O. *Inorg. Chem.* **2009**, *48*, 6960−6971.
(31) Prokofieva, A.; Prikhod'ko, A. I.; Enyedy, E. A.; Farkas, E.; Maringgele, W.; Demeshko, S.; Dechert, S.; Meyer, F. *Inorg. Chem.* **2007**, *46*, 4298−4307.
(32) Sheldrick, G. M. *Acta Crystallogr.* **2008**, *A64*, 112−122.
(33) Flack, H. D. *Acta Crystallogr.* **1983**, *A39*, 876−881.
(34) *X-RED*; STOE & CIE GmbH: Darmstadt, Germany, 2002.
(35) Wöckel, S.; Galezowska, J.; Dechert, S.; Meyer-Klaucke, W.; Nordlander, E., Meyer, F. manuscript in preparation.
(36) Addison, A. W.; Rao, T. N.; Reedijk, J.; van Rijn, J.; Verschoor, G. C. *J. Chem. Soc., Dalton Trans.* **1984**, 1349−1356.
(37) (a) Meyer, F.; Rutsch, P. *Chem. Commun.* **1998**, 1037−1038. (b) Meyer, F.; Kaifer, E.; Kircher, P.; Heinze, K.; Pritzkow, H. *Chem.—Eur. J.* **1999**, *5*, 1617−1630. (c) Siegfried, L.; Kaden, T. A.; Meyer, F.; Kircher, P.; Pritzkow, H. *J. Chem. Soc., Dalton Trans.* **2001**, 2310−2315.
(38) Hanai, K.; Maki, Y.; Kuwae, A. *Bull. Chem. Soc. Jpn.* **1985**, *58*, 1367−1375.
(39) Noncoincidence of the IR and Raman frequencies of the C═O stretch of 2-azetidinone has been explained by the presence of cyclic H-bonded dimers with a center of symmetry. The C═O vibration that is symmetric with respect to the center of symmetry is then observed at 1697 cm^{-1} in the Raman spectrum, while the asymmetric mode is observed at 1723 cm^{-1} in the IR spectrum.[38]
(40) Yang, Q.-C.; Seiler, P.; Dunitz, J. D. *Acta Crystallogr., Sect. C* **1987**, *43*, 565−567.
(41) (a) Goodgame, D. M. L.; Khaled, A. M.; O' Mahoney, C. A.; Williams, D. J. *Chem. Commun.* **1990**, 851−853. (b) Goodgame, D. M. L.; Hill, S. P. W; Williams, D. J. *Polyhedron* **1992**, *11*, 1841−1847. (c) Goodgame, D. M. L.; Hill, S. P. W; Lincoln, R.; Quiros, M.; Williams, D. J. *Polyhedron* **1993**, *12*, 2753−2762. (d) Henderson, W.; Oliver, A. G.; Rickard, C. E. F. *Inorg. Chim. Acta* **2000**, *307*, 144−148.
(42) (a) Deacon, G. B.; Phillips, R. J. *Coord. Chem. Rev.* **1980**, *33*, 227−250. (b) Zelenák, V.; Vargová, Z.; Györyová, K. *Spectrochim. Acta A* **2007**, *66*, 262−272.
(43) Asso, M.; Panossian, R.; Guiliano, M. *Spectrosc. Lett.* **1984**, *17*, 271−278.
(44) (a) Berreau, L. M. *Eur. J. Inorg. Chem.* **2006**, 273−283. (b) Natale, D.; Mareque-Rivas, J. C. *Chem. Commun.* **2008**, 425−437.
(45) (a) Zinn, P. J.; Powell, D. R.; Day, V. W.; Hendrich, M. P.; Sorrell, T. N.; Borovik, A. S. *Inorg. Chem.* **2006**, *45*, 3484−3486. (b) Graef, T.; Galezowska, J.; Dechert, S.; Meyer, F. *Eur. J. Inorg. Chem.* **2011**, 4161−4167. (c) Ng, G. K.-Y.; Ziller, J. W.; Borovik, A. S. *Inorg. Chem.* **2011**, *50*, 7922−7924.